JOURNAL OF MATERIALS SCIENCE 28 (1993) 3080–3088

Thermomechanically induced embrittlement in hot isostatically pressed Si_3N_4/SiC composites

G. PEZZOTTI
The Institute of Scientific and Industrial Research (ISIR), Osaka University, Ibaraki, Osaka 567, Japan

K. NODA, Y. OKAMOTO, T. NISHIDA
Department of Materials Engineering, Kyoto Institute of Technology, Matsugasaki, Sakyo-ku, Kyoto 606, Japan

The macroscopic fracture properties of an Si_3N_4/SiC-platelet composite fabricated by hot isostatic pressing (HIP) without sintering aids were measured by the chevron-notch technique in bending and related to micromechanisms of fracture by means of a quantitative profilometric analysis of the fracture surfaces. Compositional and processing parameters were varied systematically in order to maximize both the fracture toughness and the work of fracture of the composite. Data were compared with those of monolithic Si_3N_4 fabricated by the same process. Cooling-rate from the HIPing temperature was indicated as a critical parameter especially when cooling was performed under high pressure. A marked embrittlement of the composite body was found by cooling at around 650 °C h^{-1} and it could not be completely recovered by successive annealing even up to temperatures above 1700 °C. The highest fracture toughness and work of fracture in the composite (obtained at a cooling rate of about 100 °C h^{-1}), were measured as 4.6 MPa $m^{1/2}$ and 58.6 J m^{-2}, respectively. In agreement with fractal analysis results, they were estimated to be about 60%–70% of the maximum values, respectively, obtainable in the present composite system, provided that a complete debonding at the platelet/matrix interface can occur.

1. Introduction

A marked divergence from the linear fracture mechanics behaviour may be found in polycrystalline ceramics (1) in the presence of microstructural heterogeneities not negligibly small compared with the crack size, and (2) when internal residual stresses are developed during fabrication, so that the externally applied stress can no longer be considered as the sole cause of fracture. Both these circumstances usually occur in composites, due to geometrical and micromechanical factors. The former are generally the size, morphology, interspacing and surface roughness of the dispersed features while, among the latter ones, the internal stresses arising from anisotropy of crystal structures, phase transformations or mismatch in thermal expansion coefficients between the constituent phases have often been found to play the most significant role. All these factors combine giving rise to very complex reciprocal interactions on a microscopic scale depending on the processing conditions. Consequently, in addition, macroscopic properties such as fracture energy and fracture resistance may be found to be markedly altered.

Because of the number of microstructural parameters critically involved and their complex dependence on the processing conditions, the design of brittle/brittle composites is usually attempted empirically. It is the purpose of the present investigation, which concentrates upon one particularly simple ceramic composite system, to relate systematically the macroscopic fracture properties to the microstructural and micromechanical characteristics when compositional and processing parameters such as volume fraction of the reinforcement, cooling rate from sintering temperature and post-sintering heat treatment, are varied. A fracture mechanics technique using chevron-notched (CN) bars in bending geometry was employed for measuring the fracture energy and examining the *R*-curve behaviour of the composite bodies. On the other hand, scanning electron microscopy (SEM) followed by a three-dimensional scanning image analysis (3D SIA) provided the tools to relate the macroscopically measured fracture parameters to the micro-scale phenomena occurring during fracture.

2. Processing details and background of the composite system

The composite system selected for study was an Si_3N_4/SiC-platelet material sintered by HIP via glass-encapsulation without external addition of sintering aids, which has recently received attention in gas-turbine applications [1]. This composite was found to

0022–2461

be suitable for basic investigations because of its very simple phase composition and the "reliable" behaviour of the Si_3N_4 matrix during both sintering and fracture. In this study, composite bodies containing three different volume fractions of SiC platelets (20%, 25% and 30%; Grade M, C-Axis Technology, Jonquiere, Canada) were examined in comparison with the monolithic material also fabricated without external addition of sintering aids [2]. Monolithic and composite bodies were fabricated by the same processing and using the same starting powder (E-10, Ube Industry, Tokyo, Japan). A complete description of the fabrication process has been previously reported [1, 2]. The HIP schedule concerning temperature and pressure was varied only with respect to the cooling rate, while the top-cycle temperature/pressure (2050 °C, 180 MPa) and holding time (2 h) were maintained unchanged. The temperature was measured by a W/W–26% Re thermocouple placed inside the HIP furnace. The range of cooling rates investigated in this study was between ~500 (natural cooling) and 100 °C h^{-1} when averaged over all the temperature ranges until room temperature. However, the corresponding cooling rates between the top-cycle temperature and 1000 °C, which were constant and may be considered as the values of actual interest for covalent ceramics, were much more differentiated being the highest investigated rate of about 1100 °C h^{-1}. Only those latter values will be referred to from now on.

All the samples fabricated as described above were fully dense (> 99.5% by water-displacement method). X-ray diffraction analysis by CuK_α radiation indicated that only β-phase was present in the sintered monolithic Si_3N_4 body. Also, in the composite sintered bodies, Si_3N_4 was detected only as β-phase, indicating a complete transformation from the alpha starting powder. On the other hand, no peaks for β-SiC were detected in the starting platelets, nor in the sintered composites. A quantitative plot of the number of interceptions per unit length counted in various planes inside the composite specimens showed that the SiC platelets were randomly arranged in the matrix up to 30 vol % addition [3].

It is known that the grain boundary in monolithic Si_3N_4 and in Si_3N_4/SiC composites [4, 5] sintered by HIP without external addition of sintering aids is constituted by a thin glassy SiO_2 film which is present as an impurity of about 2.4 wt % in the starting Si_3N_4 powder. Neither microcracking nor crystallization of the SiO_2 glassy phase at the grain boundary were detected by transmission electron microscopy observation (TEM) for any of the investigated cooling rates. The morphology of the grain boundary was found to be very similar after either slow or fast cooling, the observed thickness being between 1 and 4 nm. A clear halo pattern was systematically detected at the triple points proving the non-crystalline structure of the intergranular phase. Cracking was not observed inside the SiC platelets. However, a high density of stacking faults and partial dislocations was detected. The stacking-fault structure was also observed in the starting platelets, while the dislocations were introduced by sintering and their density was higher in composite specimens subjected to slow cooling. On the other hand, no planar faults were observed in the Si_3N_4 grains and no difference was noticed in their crystal structure, though their average size (about 1 μm) was smaller, in agreement with a shorter duration at high temperature. Detailed TEM observations of the present composite microstructures are reported elsewhere [6].

Analyses of the room-temperature fracture in the monolithic material [7] as well as in composites [8] showed that the Si_3N_4 grains fractured transgranularly because of a strong bonding operated by the SiO_2 glassy phase at the grain boundary. Consequently, as shown in details later, the fracture energy of the present matrix was found to be very close to that of a Si_3N_4 single-crystal. Because of the marked transgranular nature of fracture in the present Si_3N_4, which makes its fracture energy almost independent of the grain size and morphology, eventual differences between the matrix microstructures which may arise from the presence during sintering of the SiC-phase, will be considered to have a negligible influence in the present composite system.

3. Fracture mechanics analysis

3.1. Experimental and analytical details

The determination of fracture energy and *R*-curve behaviour both in monolithic and composite materials was carried out in bending fracture tests on bars 2 mm × 3 mm × 50 mm in dimensions. The bars were cut to obtain a chevron notch of 90° angle in the specimen centre. The notches had a slot width of 0.15 mm and the resulting ligament area was about 1.9 mm^2. The specimens were loaded to achieve stable fracture in three-point bending with a span of 45 mm under a crosshead speed of 0.002 mm min^{-1}. The areas subtended by the recorded load–deflection curves were divided by double the amount of the respective ligament areas to provide the work of fracture (WOF) values. Then, after subtracting the deflection of the bending machine, which was previously measured by a blank test, the curves were analysed by the compliance method to obtain the characteristic relations between crack resistance, K_R, and crack length, Δa. The following set of five equations was employed for the analysis [9, 10]

$$C = \int_0^\alpha (9S/2E'BW^2)\,\alpha Y^2(\alpha)\,d\alpha + C_0 \quad (1)$$

$$C_0 = (1/EB)(S/W)^2\{[S/4W] + [(1+\nu)W/2S]\} \quad (2)$$

$$a = a_0 + \Delta a \quad (3)$$

$$K_R = (3PS/2BW^2)\,a^{1/2}Y \quad (4)$$

$$Y = (S/W)[3\alpha^{1/2}/2(1-\alpha)^{3/2}] \times \{1.9887 - 1.326\alpha - [(3.49\alpha - 0.68\alpha^2 + 1.35\alpha^3)(1-\alpha)/(1+\alpha^2)]\} \quad (5)$$

where E' and ν are Young's modulus and Poisson's ratio of the material, the geometrical parameters B, W,

$C(\alpha)$ and C_0 are the specimen thickness, width, compliance during fracture and compliance without notch, respectively. P is the applied load, Y the shape factor for the present testing geometry and S is the bending span. The relative crack length, α, is calculated from the ratio between the crack length, a, and the specimen width, W, while a_0 is the notch length, Δa is the crack extension from the notch apex. Crack initiation was detected by an acoustic emission detector directly attached to the bending bar. Further details about the testing procedure are described elsewhere [11].

3.2. Results

Although no macroscopic specimen cracking due to thermal shock was observed even in the case of natural cooling from the top-cycle temperature, a wide scattering of data was found in the case of very fast cooling rate, depending upon the location of the cut bending bar inside each single composite specimen. This was thought to be a phenomenon related to the non-homogeneous distribution of temperature during cooling inside the HIPed specimen which usually consisted of a rod with a diameter (after sintering) of about 30 mm. At cooling rates of about 650 °C h^{-1}, such a phenomenon was significantly attenuated and each HIPed specimen showed almost uniform fracture properties. The influence of the macroscopic temperature gradient inside the specimen on the heterogeneity of its fracture properties will not be investigated in the present report which focuses on the effect of the processing conditions on the microfracture behaviour of the materials. Therefore, only experiments in the range 650–100 °C h^{-1} will be discussed in detail, the cooling rates at around 650 and 100 °C h^{-1} usually being referred to as "fast cooling" and "slow cooling", respectively.

When the cooling rate is appropriately scheduled, the presence of 25 vol % SiC platelets in the Si_3N_4 matrix can lead to a significant improvement of the fracture energy, as well as the crack resistance of the material. This is clearly shown in Fig. 1a and b. A WOF up to six times larger than that of monolithic Si_3N_4 was measured due to dissipative phenomena operating both at the tip and in the wake of the propagating crack. The wake contribution is confirmed by the rising R-curve behaviour of the composite in comparison with the flat behaviour of the matrix. The contributions by crack-tip and crack-wake phenomena to the increase in fracture energy of the composite may be shared in the present experiments. Considering that, in the load–displacement curves (Fig. 1a), the top load corresponds to the K_R at minimum crack length in Fig. 1b (assumed as the K_{Ic} of the material), an increase of such a parameter will represent the effect of mechanisms operating at the instantaneous front of the crack as, for example, debonding at the interface and pinning by platelets. On the other hand, the slope of the decreasing load–displacement curve after critical loading which is related to the rising R-curve behaviour of the material, reflects the amount of energy dissipated in the wake of the crack by friction and bridging phenomena. Regarding the present results from the above point of view, a quantitative analysis of the microfracture behaviour will be attempted later.

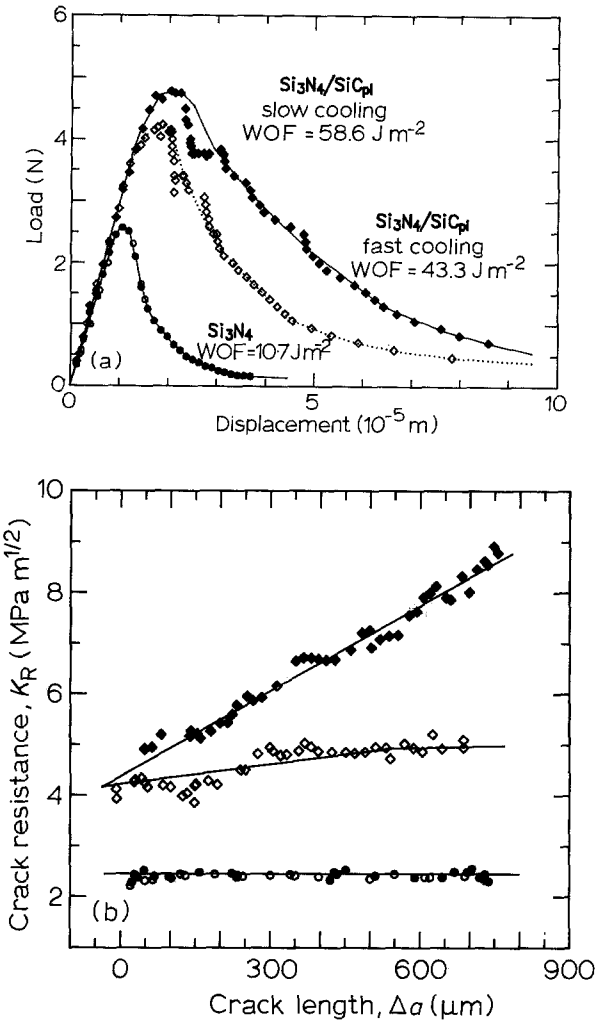

Figure 1 Load–displacement curves (a) after subtracting the machine compliance and (b) R-curve behaviour as detected in monolithic and 25 vol % SiC-platelet composite for different cooling rates from the HIPing temperature. (○, ◇) Fast cooling, (●, ◆) slow cooling.

Although the cooling-rate parameter, in the case of HIP sintering, did not affect the fracture behaviour of the present monolithic Si_3N_4, it had a marked influence on that of the Si_3N_4/SiC composite. Fig. 1 also shows the embrittlement caused in composites by a "fast" cooling which leads to a decrease in K_{Ic} and a flat R-curve behaviour. In other words, a diminution is found in the effectiveness of crack-tip mechanisms as well as in the crack-shielding forces operated by the platelets behind the crack-front. In addition, this result was found to be independent of the amount of SiC platelets up to 30 vol % content, as shown in Fig. 2.

Systematic annealing experiments were then conducted on the "brittle" composite specimens. Composite bars cut from the HIP specimen subjected to fast cooling, were annealed in a nitrogen atmosphere (30 Pa) for 6 h in a range of temperatures between 1200 and 1750 °C. No weight-loss was detected after annealing. A consistent finding was that, for any annealing temperature less than 1700 °C, no modification of fracture behaviour was found. However, in the range of temperature between 1700 and 1750 °C, a

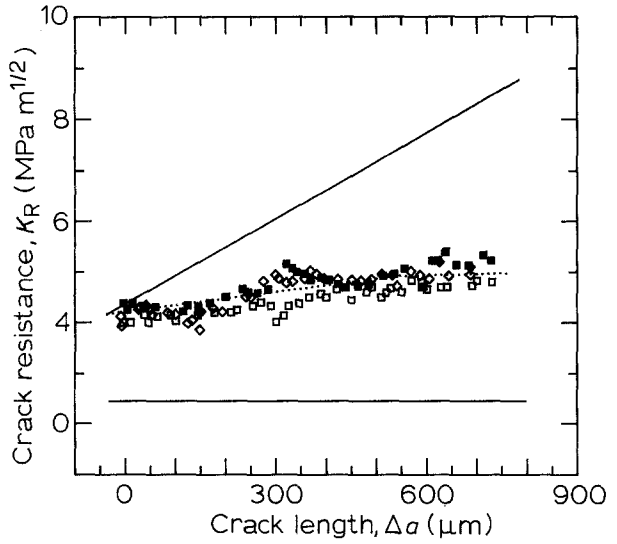

Figure 2 Effect of volume fraction of SiC platelets on the *R*-curve behaviour of the present composite in case of "fast cooling" from the HIPing temperature. (◇) Si_3N_4/20% SiC_{pl}, (◇) Si_3N_4/25% SiC_{pl}, (■) Si_3N_4/30% SiC_{pl}.

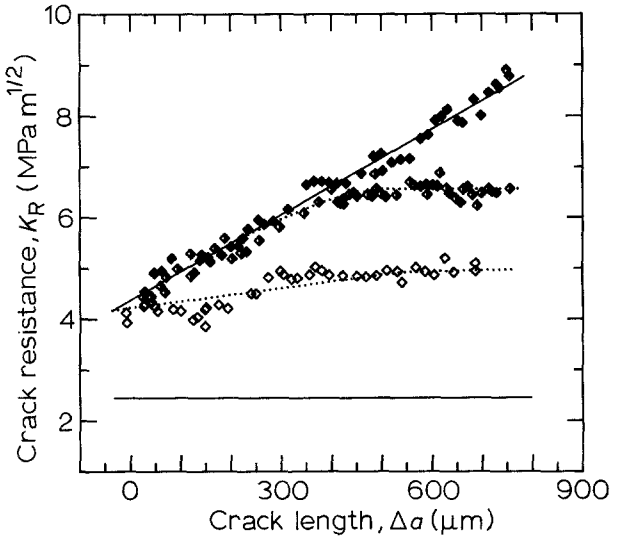

Figure 3 Effect of post-HIPing annealing process at 1750 °C in a nitrogen atmosphere on the *R*-curve behaviour of Si_3N_4/25 vol % SiC-platelet composite. (◆) slow cooling, (◇) fast cooling, (◈) annealing at 1750 °C.

partial recovery of the fracture resistance was detected with increasing crack-length. As a typical pattern, Fig. 3 shows the results obtained after annealing at 1750 °C in 25 vol % composite. In addition, the cooling rate of the annealing cycle which was varied in the same range of that of the HIP cycle, was not found to be affecting such a recovery process. In addition to the possible important implications of this latter result, which will be discussed in a successive section, it should be noted that a direct comparison between the cooling rates of HIP and annealing cycles may not be reliable, because the thickness of the composite specimens during the latter cycle was about ten times smaller than that during HIPing.

4. Quantitative fractography

SEM images of the fracture surfaces of CN bars are shown in Fig. 4a and c. They show the composite specimens cooled down at 100 and 550 °C h^{-1}, respectively. There is a clear difference in surface roughness between these two materials, as better revealed by higher magnification micrographs (Fig. 5a and c). A large percentage of SiC platelets in the "quenched" composite was found to be fractured straight away, even when oriented at low angles with respect to the main crack plane. In other words, the debonding length at the Si_3N_4/SiC interface was significantly reduced by fast cooling. This observation was proved quantitatively by the profilometric analysis of the fracture surfaces. Fracture profiles were generated on the scanning electron micrographs by means of a 3D SIA (as shown, for example, in Figs 4b–d and 5b–d) and analysed with respect to their length. The inter-CN fracture surfaces of specimens fabricated at different cooling rates or after annealing at 1750 °C were automatically examined. On increasing the magnification of the SEM images, the profile lengths of various specimens became markedly different. Furthermore, important details regarding the micromechanical interaction between the propagating crack and the platelets were revealed by analysis at high magnification. Fig. 6 represents the SEM image of a fractured SiC platelet and the results of the fractographic analysis. The analysis was performed along the two lines indicated by arrows on the scanning electron micrograph and revealed both the orientation of the platelet and the debonding length. It is interesting to note that the crack path inside the platelet is generally not flat unless, in addition, cleavage fracture could be observed depending upon the reciprocal orientation between platelet and main crack. This characteristic was confirmed by observing the crack profiles generated by a Vickers indentation of 50 kg on the lapped surface of a composite body (Fig. 7). It was found that when the main crack was not parallel to an SiC cleavage plane, debonding at the interface generally occurred without any apparent relation to the platelet thickness. Then, the crack tip could enter successively into the platelet (Fig. 7a) or a complete debonding could occur (Fig. 7b). Frequently, the main crack was observed running in the matrix from a stress accumulation point downstream of the platelet. Even when cleavage fracture occurs (Fig. 7c), debonding could be observed at the successive interface. Cleavage planes were generally found non-parallel to the platelet thickness.

The quantitative results of this extensive fractographic analysis are summarized in Fig. 8 in terms of profile roughness (ratio between the measured profile length and its projection on the fracture plane). The raw data as a function of the measuring unit are plotted in Fig. 8a. The curves obtained showed a typical sigmoidal shape which was linearized by the log–log plot of Fig. 8b, as suggested by Underwood and Banerji [12] and as usually adopted in phase-transformation studies. The constant R_L^0, which represents the "true" length of the profile (asymptotic limit of length as the measuring unit approaches zero), was determined graphically after fitting the data of Fig. 8a. After linearization, the curves are easily characterized by the parameter $\Delta^* = 1 + \beta$ which represents their

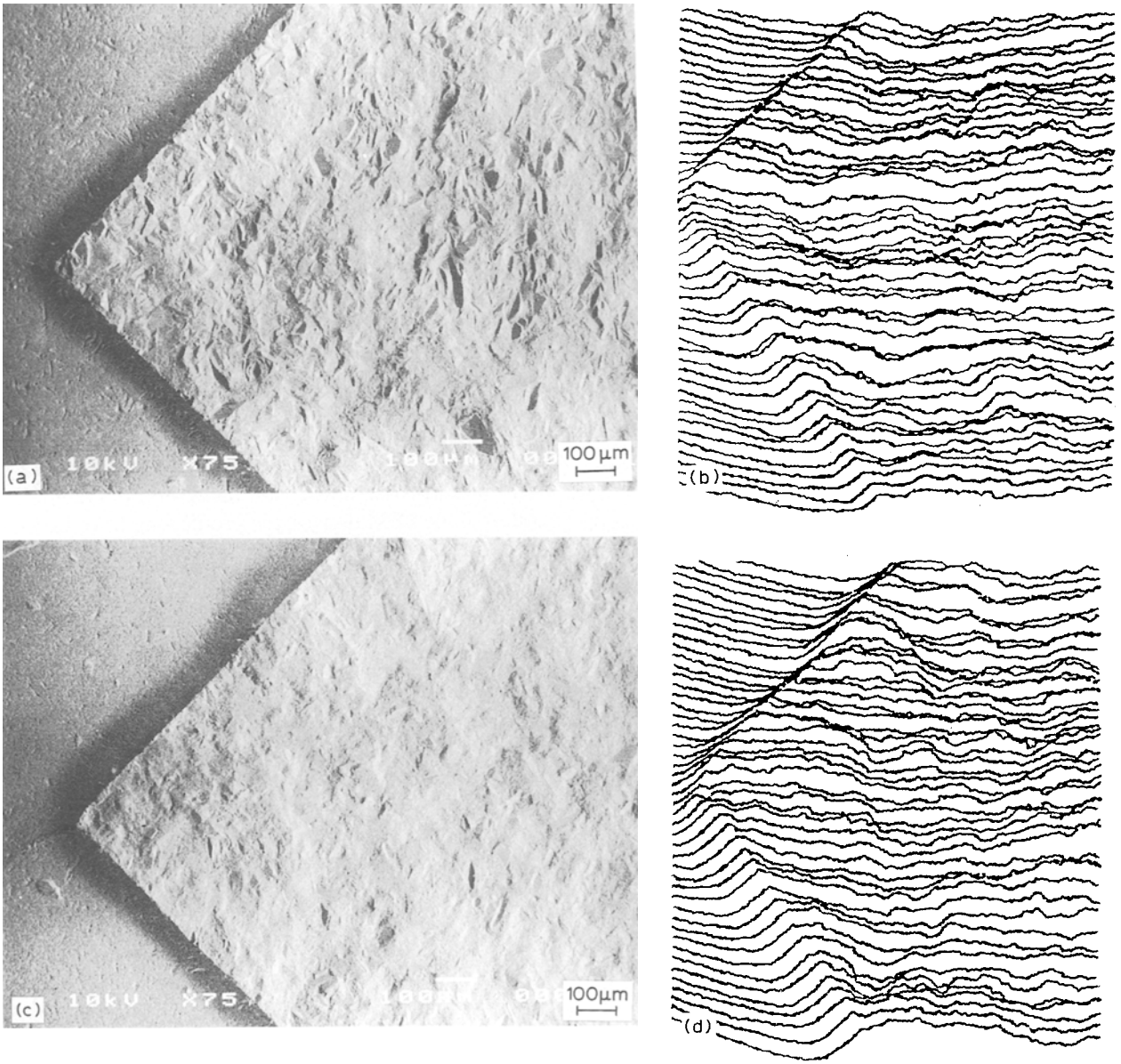

Figure 4 SEM images of CN fracture surfaces and their respective 3D SIA profiles for Si_3N_4/25 vol % SiC-platelet composites cooled from HIPing temperatures at (a, b) 100 °C h^{-1}, and (c, d) 650 °C h^{-1}.

modified fractal dimension [12, 13]. β is the slope of the linear plot which was obtained graphically from Fig. 8b. Although it is not easy to relate to each other the fractal dimensions of monolithic and composite materials, the composite pattern seems to be suitable for a rational interpretation. First, it is recognized that the straight lines start approximately from the same origin and have different slopes which increase with decreasing brittleness of the material. The roughness data relative to the specimens subjected to slow and fast cooling, start to be clearly differentiated below a measuring unit of about 50–10 µm, a fact which quantifies the characteristic length of the microfracture mechanism and confirms the hypothesis of a direct dependence of the interface debonding length on the cooling rate. Furthermore, both K_{Ic} and WOF of the various composites were found to be related to the fractal dimension, Δ*, by a simple linear relation (Fig. 9). Therefore, if we assume that in all the present composite specimens the toughening mechanisms (seen here as sources of energy dissipation and operating either at the crack tip or in the crack wake) are basically the same, even acting with different intensities, it is found that their effectiveness is actually "memorized" after fracture in the fracture surface itself and can be promptly read by its fractal dimension. This concept will be used in the next section for estimating by extrapolation the maximum toughening achievable by platelet reinforcement in the present composite system.

5. Discussion

5.1. Relations between HIP process and fracture behaviour

Several indications linking the HIP process and the fracture behaviour of Si_3N_4/SiC composite, have been reached in the present investigation. First of all, it is found that the cooling from sintering temperature, especially when conducted under high pressure, plays a key role in the final properties of the composite.

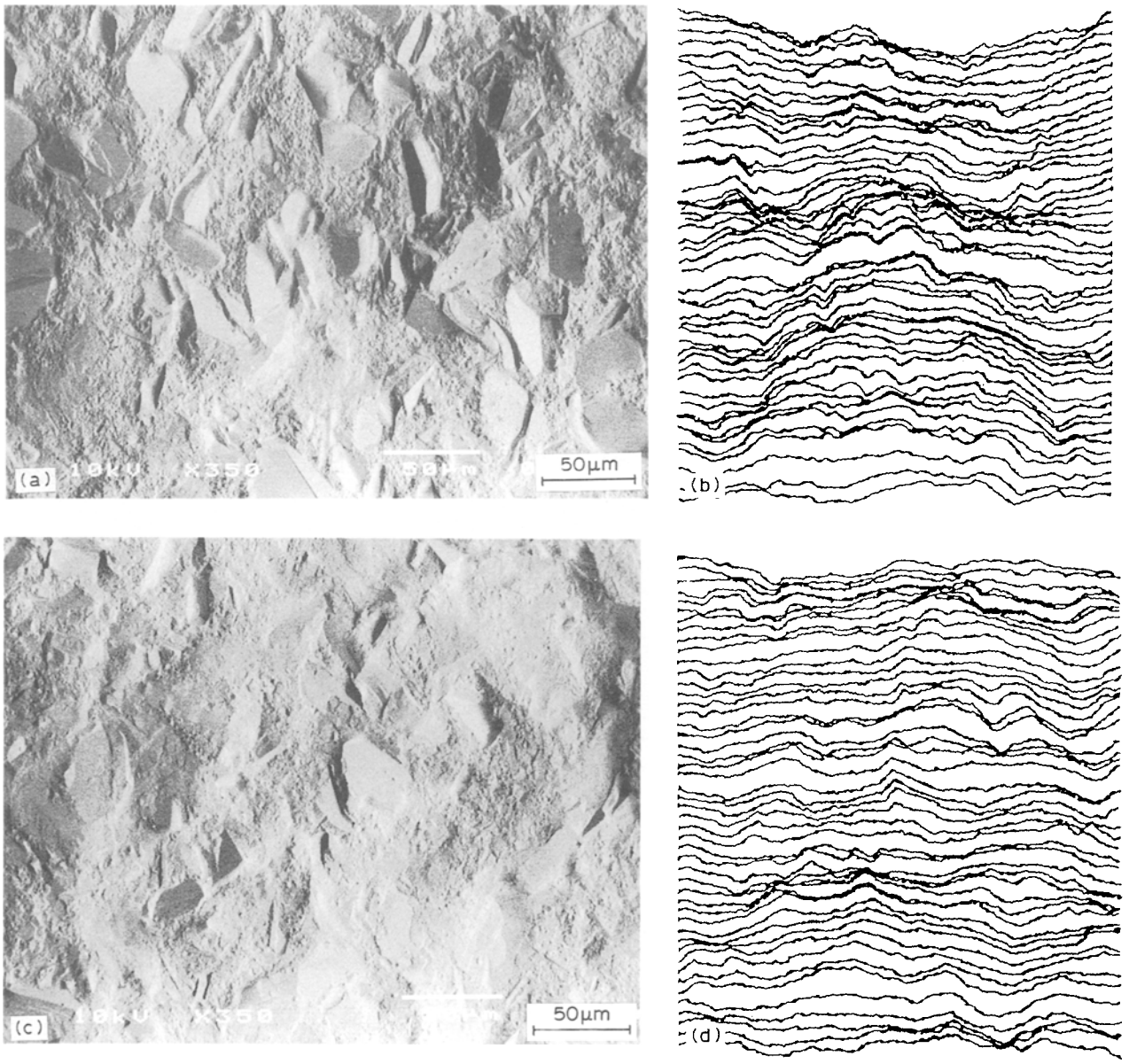

Figure 5 SEM images and 3D SIA analysis at higher magnification for composite specimens. Cooling conditions and respective notations are the same as those in Fig. 4.

Cooling rates, as generally adopted in ceramic technology, and annealing temperatures at around 1200 °C, which are usually believed to be appropriate to release internal stresses in ceramics, were not suitable for the present composite system. This trend may be somehow general for highly refractory ceramic composites by HIP. It should be emphasized, however, that high pressure is required in sintering Si_3N_4/SiC composites without additives which cannot otherwise be fully densified. On the other hand, the present work may suggest that, after achieving the desired relative density, cooling without pressure is the most suitable for composites. Unfortunately, such experiments cannot be easily performed due to the technological problem of evacuating highly pressurized argon gas at around 2000 °C from the HIP furnace. It is believed that the high annealing temperature ($\geqslant$ 1700 °C) needed to recover, even only partially, the embrittlement by HIP fast-cooling, is related to the necessity of a re-softening of the intergranular glassy SiO_2 phase which has a high purity and melts at about 1730 °C [2]. Data from quantitative fractography indicated that the per cent of immediate cleavage fracture of SiC platelets increased (i.e. the debonding length was significantly reduced) when composite cooling was performed at a fast rate. On the other hand, no difference either in the grain-boundary morphology or composition was detected by TEM in composites processed by different cooling rates. Considering also that no internal cracking was observed inside the SiC platelets, the embrittlement by fast cooling of the present composite system can be thought of as due to (1) an increase in interfacial bonding strength between Si_3N_4 and SiC, as well as (2) a change in the microscopic fracture resistance of the SiC platelets with the processing conditions. According to the above former hypothesis, an improved bonding may be due to residual stress at the matrix/reinforcement interface. However, it is clear that this stress is not elastic in nature. Elastic residual stresses due to mismatch in thermal expansion coefficient between matrix and reinforcement, should be in tension on the platelets and tend to weaken the interface, the thermal expansion coefficient of the reinforcement being larger than that of the matrix. Further-

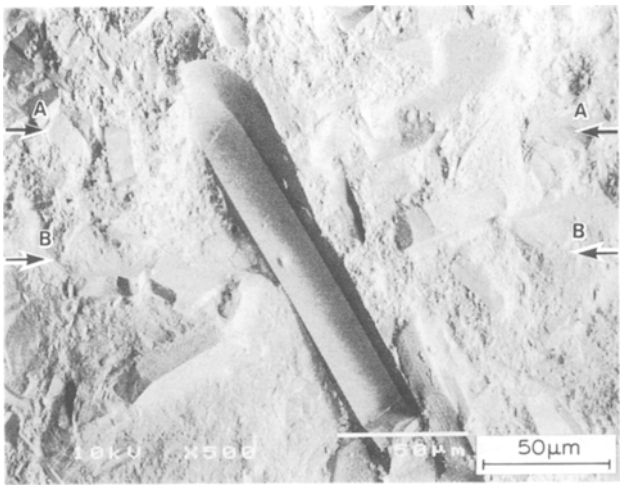

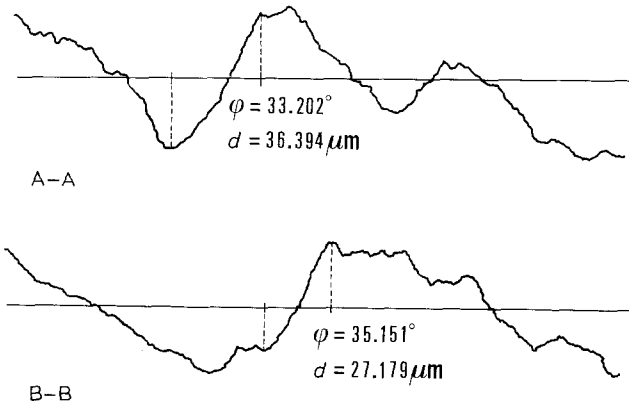

Figure 6 Details of high-magnification profilometric three-dimensional analysis of the interaction between a crack and an SiC-platelet. A complete characterization of the local fracture phenomenon can be performed. As an example, the analysis is shown scanning the two lines indicated by arrows.

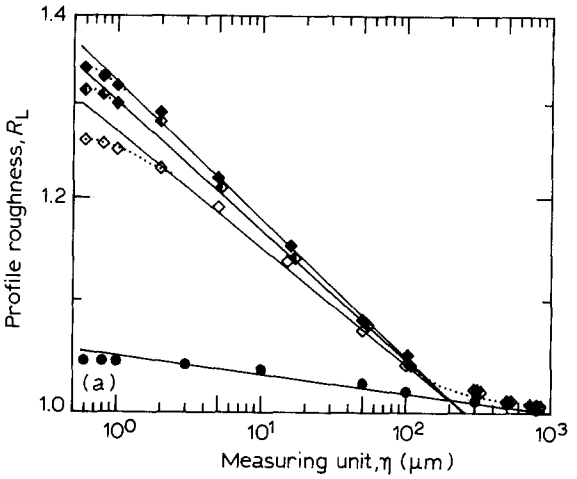

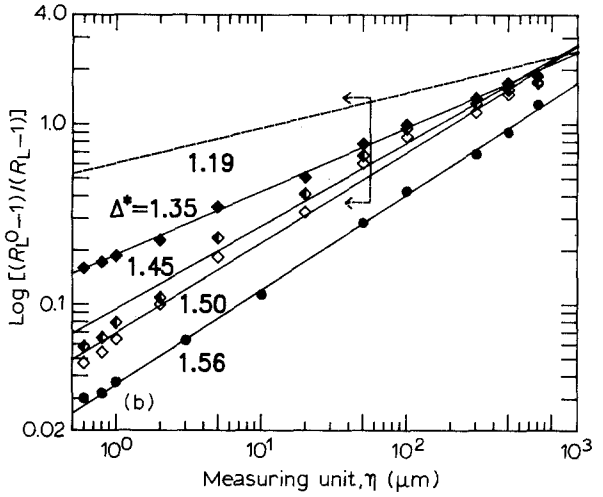

Figure 8 Sigmoidal dependence of (a) the profile roughness and (b) their "linearized" patterns, as a function of the measuring unit for monolithic Si_3N_4 and various composite specimens (Si_3N_4/25% SiC_{pl}). (◇) slow cooling, (◆) fast cooling, (◐) annealing at 1750 °C, (●) monolithic Si_3N_4.

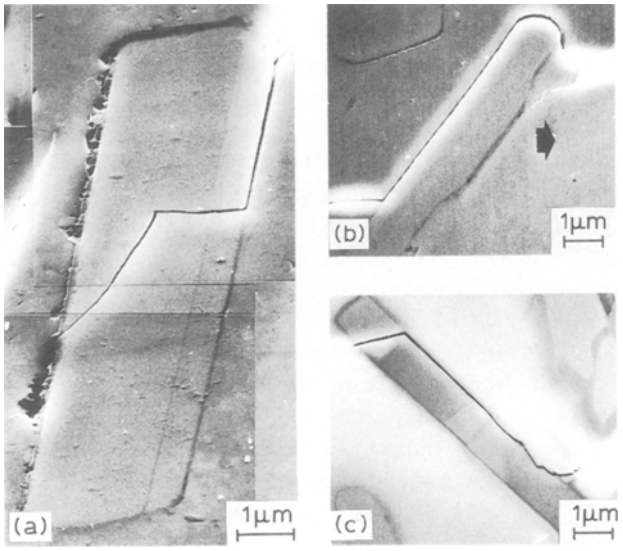

Figure 7 Scanning electron micrographs of crack profiles generated by Vickers indentation on the lapped surface of a composite specimen cooled from the HIPing temperature at 100 °C h^{-1}.

more, elastic residual stresses should not be affected by time-dependent parameters such as the cooling rate. From a phenomenological point of view, it seems that a "frozen" compressive interfacial stress due to the high applied pressure, remains stored in the composite when the sintered body is rapidly cooled which is a well-known phenomenon in glass-based materials [14]. Further studies should be performed to ascertain whether or not "frozen" stresses can remain in HIPed ceramics, as well as to relate the micromechanical behaviour of the platelets to their crystal structure after sintering.

5.2. Maximum toughness achievable in the Si_3N_4/SiC-platelet system

It is shown by the above results that an optimization of the HIP-process parameters (especially cooling rate and applied pressure) and/or (post-HIPing) annealing process, may lead to an improvement of the fracture behaviour of highly refractory composites. It would be expedient, then, to attempt an evaluation of the maximum toughening achievable by SiC platelets in the present composite system according to fractal analysis results. When fracture is completely transgranular in the matrix but a complete debonding can occur around disc-shaped platelets randomly distributed inside the matrix, the fracture profile morphology leads

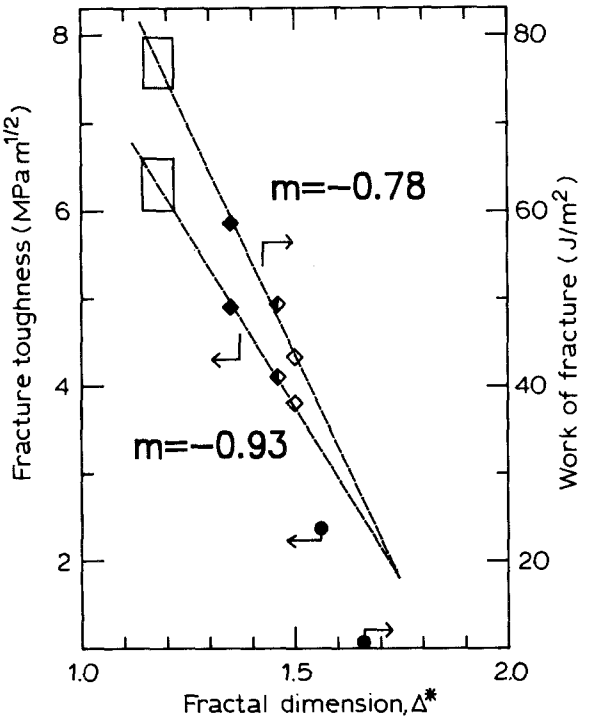

Figure 9 Dependence of fracture toughness and WOF on the fractal dimension of the CN fracture surfaces for monolithic and various composite sintered bodies. The notations are the same as those in Figs 1–3. The calculated slopes of the linear relationships found in the composite system are also indicated.

to a profile roughness

$$R_L = 1 + [(H + t)/I] - \{[t/I(\pi/2 - \theta_L)] \int_{\theta_L}^{\pi/2} (1/\tan\theta)\, d\theta\} \quad (6)$$

where H, t and I are the platelet diameter, thickness and centre-to-centre near-neighbours distance, respectively, θ is the acute angle between the platelet and the main fracture plane which can randomly vary in the interval $[\pi/2, \theta_L]$. In a previous report [3], the mean shape and interspacing between platelets in the present composite system were evaluated by image analysis techniques. It was found that the average shape of the platelets was a disc with average diameter and thickness of 26.2 and 3.2 μm, respectively. Data of centre-to-centre near-neighbours distance as a function of the volume fraction of platelets are plotted in Fig. 10 together with the values of profile roughness, R_L, respectively calculated from Equation 6. In the calculation, the lower boundary of integration was assumed as $\theta_L = \pi/90$. The roughness values measured in the present materials are also plotted for comparison. Considering the calculated values of R_L as those corresponding to a measuring unit $\eta = 3$ μm, which is approximately the average platelet thickness (i.e. smallest profile segment counted up in the calculation), the predicted fractal dimension in the case of complete debonding around the platelets in the 25 vol % composite, is $\Delta^* = 1.19$ (dotted line in Fig. 8). Extrapolating from the slopes of Fig. 9, a maximum fracture toughness, $K_{Ic} = 6$–7 MPa m$^{1/2}$ and WOF $= 75$–80 J m^{-2} can be calculated for platelet contents

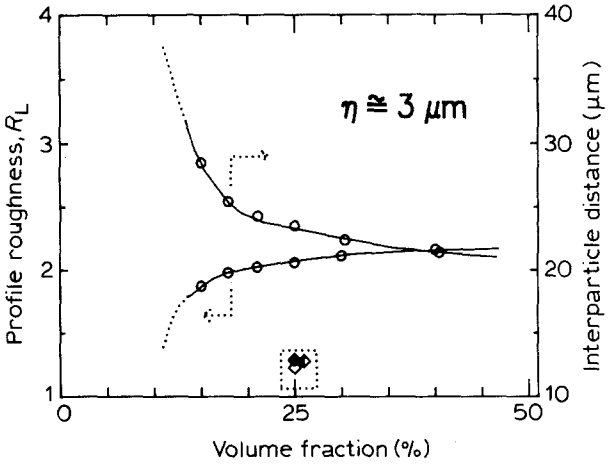

Figure 10 Interparticle distance and the respective calculated profile roughnesses as a function of the volume fraction of platelets in the composite sintered body. Experimental data are also shown for comparison.

between 15 and 40 vol % (□ in Fig. 9). It is noteworthy that a back-calculation from Fig. 10 indicates complete crack-tip debonding only corresponding to a relatively small fraction of platelets (about 10 vol %) in the present composite.

6. Conclusion

The present study provides characterization of the macroscopic fracture properties of Si_3N_4/SiC-platelet composite and relates them to the micromechanical fracture processes when compositional and processing parameters are varied. The Si_3N_4/SiC composites sintered by HIP without sintering aids showed a fracture behaviour markedly dependent upon the cooling rate after HIP sintering. According to a quantitative profilometric analysis of the fracture surfaces after CN experiments, the embrittlement found after fast cooling ($\sim 650\,^\circ$C h^{-1}) under an isostatic pressure of 180 MPa was associated with a decrease in debonding length at the platelet/matrix interface. The embrittlement was only partially recovered by annealing at temperature exceeding 1700 °C. Furthermore, the cooling rate after the annealing process did not affect the final fracture properties of the composite. The decrease in debonding length was thought to be related to a compressive microstress thermomechanically induced at the Si_3N_4/SiC interface during fast cooling under high pressure and/or to a lower microfracture strength of the platelets. The highest toughness in the present composite was achieved by cooling at 100 °C h^{-1}. K_{Ic} and WOF were, respectively, improved by about 85% and 450% over the matrix values. In agreement with fractal concepts, further increases of about 40% and 200% of K_{Ic} and WOF, respectively, are predicted when a complete debonding at the platelet/matrix interface is obtained via optimization of the HIP process conditions.

Acknowledgements

One of the authors (G.P.) was financially supported by the Japan Society for the Promotion of Science (JSPS).

The authors thank Professor T. Urabe and Miss K. Saito, Ryukoku University, for the SIA experiments, and Professor K. Niihara for providing the research facilities at ISIR, Osaka University.

References

1. G. PEZZOTTI, *J. Amer. Ceram. Soc.* submitted.
2. I. TANAKA, G. PEZZOTTI, T. OKAMOTO, Y. MIYAMOTO and M. KOIZUMI, *ibid.* **72** (1989) 1656.
3. G. PEZZOTTI, *Acta Metall. Mater.*, submitted.
4. I. TANAKA, G. PEZZOTTI, K. MATSUSHITA, Y. MIYAMOTO and T. OKAMOTO, *J. Amer. Ceram. Soc.* **74** (1991) 752.
5. G. PEZZOTTI, I. TANAKA and T. OKAMOTO, *ibid.* **73** (1990) 3033.
6. G. PEZZOTTI and T. NISHIDA, *Yogyo Kyokaishi*, submitted.
7. I. TANAKA, G. PEZZOTTI, Y. MIYAMOTO and T. OKAMOTO, *J. Mater. Sci.* **26** (1991) 208.
8. G. PEZZOTTI, I. TANAKA and T. OKAMOTO, *J. Amer. Ceram. Soc.* **73** (1990) 3039.
9. D. MUNZ, R. T. BUBSEY and J. L. SHANNON Jr, *ibid.* **63** (1980) 300, Appendix.
10. F. WAKAI, S. SAKAGUCHI and Y. MATSUNO, *Yogyo Kyokaishi* **93** (1985) 479.
11. G. PEZZOTTI and T. NISHIDA, *ibid.*, submitted.
12. E. E. UNDERWOOD and K. BANERJI, *Mater. Sci. Engng* **80** (1986) 1.
13. *Idem*, in "Fractography" Vol. 12 (ASM, Metals Park, OH, 1987) p. 211.
14. U. C. PAEK and C. R. KURKJIAN, *J. Amer. Ceram. Soc.* **58** (1975) 330.

Received 10 July
and accepted 4 August 1992